

Controlling the Dynamics of an Open Many-Body Quantum System with Localized Dissipation

G. Barontini,* R. Labouvie, F. Stubenrauch, A. Vogler, V. Guarrera, and H. Ott

Research Center OPTIMAS and Fachbereich Physik, Technische Universität Kaiserslautern, 67663 Kaiserslautern, Germany
(Received 4 October 2012; revised manuscript received 28 November 2012; published 15 January 2013)

We experimentally investigate the action of a localized dissipative potential on a macroscopic matter wave, which we implement by shining an electron beam on an atomic Bose-Einstein condensate (BEC). We measure the losses induced by the dissipative potential as a function of the dissipation strength observing a paradoxical behavior when the strength of the dissipation exceeds a critical limit: for an increase of the dissipation rate the number of atoms lost from the BEC becomes lower. We repeat the experiment for different parameters of the electron beam and we compare our results with a simple theoretical model, finding excellent agreement. By monitoring the dynamics induced by the dissipative defect we identify the mechanisms which are responsible for the observed paradoxical behavior. We finally demonstrate the link between our dissipative dynamics and the measurement of the density distribution of the BEC allowing for a generalized definition of the Zeno effect. Because of the high degree of control on every parameter, our system is a promising candidate for the engineering of fully governable open quantum systems.

DOI: [10.1103/PhysRevLett.110.035302](https://doi.org/10.1103/PhysRevLett.110.035302)

PACS numbers: 67.85.Hj, 03.75.Gg, 34.80.Dp

Gathering information from a quantum system is never free of cost. Every measurement process provides a coupling between the quantum system and the (classical) environment, which leads to nonunitary dynamics, and in some cases to the destruction of essentially quantum effects. The elusive transition from the quantum to the classical realm must therefore be inherent in the processes that the environment induces on the system. In recent decades several advances have been made in the study of environmentally induced phenomena like decoherence and decoherence-induced selection of preferred states (einselection) [1–3]. More recently environmental action has been used to manipulate qubits in a system of trapped ions [4]. The knowledge and the mastering of the action of the environment are essential for taming errors in quantum computation schemes [5,6] or to engineer decoherence-free subspaces for qubits [7–9], and are also key to understanding the emergence of classicality from the quantum [2,3]. In the context of the theory of open quantum systems, environmental action gives rise to effective Hamiltonians which can contain imaginary terms [2,3,10]. Since these terms actually arise from a collection of an enormous number of degrees of freedom [3], however, a complete experimental control over them appears overly challenging. Here, we report the engineering of a fully controllable, environmentally induced imaginary potential acting on a quantum system, and present observations of the subsequent induced dynamics. The localized imaginary potential is realized by the almost pure dissipative action of an electron beam (EB) on an atomic Bose-Einstein condensate (BEC). We show that such a potential can be used to describe a continuous measurement process that can exhibit a generalized version of the so-called Zeno effect. The combination of the robust and macroscopic

many-body quantum behavior of a BEC and the high tunability and precision of the EB promotes such a system as a paradigm for governable open quantum systems.

One of the most striking properties of BECs is that, despite their many-body nature, they can be described to a good approximation by a mean-field wave function obeying the so-called Gross-Pitaevskii equation (GPE). This remains valid also when the BEC is coupled with the environment. Starting from the Lindblad master equation $i\hbar\partial_t\hat{\rho} = [\hat{H}, \hat{\rho}] + i\hbar\hat{\mathcal{L}}\hat{\rho}$, where $\hat{\rho}$ is the density operator of the many-body system, \hat{H} is the Hamiltonian operator, and $\hat{\mathcal{L}}$ is the dissipation operator such that $\hat{\mathcal{L}}\hat{\rho} = -\int d\mathbf{x}\gamma(\mathbf{x})/2[\hat{\Psi}^+\hat{\Psi}\hat{\rho} + \hat{\rho}\hat{\Psi}^+\hat{\Psi} - 2\hat{\Psi}\hat{\rho}\hat{\Psi}^+]$, with $\gamma(\mathbf{x})$ the local dissipation rate, we can write the equation of motion for the expectation value of the bosonic field operator $\hat{\Psi}$ as $\partial_t\langle\hat{\Psi}\rangle = \text{Tr}(\hat{\Psi}\partial_t\hat{\rho})$, which leads to a time-dependent GPE with an additional imaginary term (see the Supplemental Material [11] and Refs. [12,13]):

$$i\hbar\frac{\partial\psi(\mathbf{x},t)}{\partial t} = \left(-\frac{\hbar^2\nabla^2}{2m} + V_{\text{ext}} + g|\psi(\mathbf{x},t)|^2 - i\hbar\frac{\gamma(\mathbf{x})}{2}\right)\psi(\mathbf{x},t). \quad (1)$$

Here ψ is the BEC wave function, obeying the constraint $\int|\psi(\mathbf{x},t)|^2d\mathbf{x} = N(t)$, V_{ext} is the trapping potential, and $g = 4\pi\hbar^2a/m$, a being the s -wave scattering length. Notably our technique allows independent control of the Hamiltonian and dissipative terms of this equation. The ability to describe our open quantum many-body system with such a simple expression is a key asset for understanding and mastering its dynamics.

Experimental implementation.— In our experiment we prepare a pure BEC of 75×10^3 atoms in a single-beam optical trap by means of forced evaporation. Once the

evaporation is over, we shine a focussed EB right at the center of the BEC. The EB is produced by a commercial electron microscope mounted inside the vacuum chamber [14]. The electron microscope is able to generate a beam of 6 keV electrons with variable beam extensions and currents. When the electrons impact on the BEC they collide locally with the atoms, ionizing or exciting them. Those atoms which have undergone an electron collision escape from the trapping potential [see Fig. 1(a)]. The EB thus locally dissipates the BEC. The ionized atoms, roughly 40% of all those scattered, are then directed to an ion detector, where their arrival times are registered. While escaping from the trapping region the ions can collide with the trapped atoms producing additional losses [11]. The total detection efficiency η is the product of the branching ratio (40%) and of the combined ion optics and detector efficiency (75%). Details of the experimental apparatus can be found in Refs. [14,15]. If the EB is rapidly moved in a controlled pattern, the whole column density profile of the BEC can be reconstructed [14,16]. Here we keep the EB fixed in the center of the BEC, and monitor the subsequent induced dynamics by looking at the temporal signal from the ion detector [see Fig. 1(b)]. By controlling the beam parameters, we can engineer the dissipative term in Eq. (1): we write it as $\gamma(\mathbf{x}) = I\sigma/(2\pi ew^2) \exp(-(x^2 + y^2)/2w^2)$, I being the EB current, σ the electron-BEC scattering cross section [11], e the elementary charge, and w the standard deviation of the spatial electron distribution, assumed to be Gaussian [11].

Comparison between experimental results and theoretical expectations.— In Fig. 2 we report the number of ions collected in the first 5 ms of continuous dissipation as a function of the EB current for three different values of w . Notably we observe that the number of ions produced, as a function of the EB current (i.e., of the number of electrons sent on the atoms), shows a nonmonotonic dependence. In other words, starting from a critical value of the EB current, the harder we try to dissipate, the less we manage to do it.

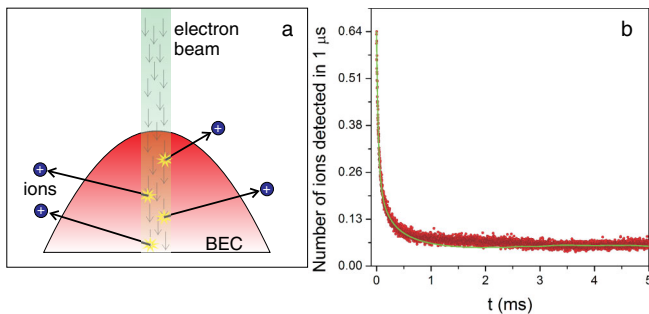


FIG. 1 (color online). (a) The electrons locally collide with the atoms constantly dissipating the BEC. (b) Temporal resolved signal from the ion detector. The bin size is $1 \mu\text{s}$. Points are experimental data averaged over 1800 experimental repetitions, while the solid curve is the numerical simulation (see text). After 5 ms we typically collect ≈ 450 ions.

This paradoxical behavior is more marked for smaller values of w . In the same figure the data are compared with the results obtained by numerically solving Eq. (1), additionally taking into account secondary effects like ion-atom collisions [11]. The agreement is very good [and the same agreement is visible in Fig. 1(b)], demonstrating that the description of the EB as a pure dissipative potential is sufficient to capture the observed main features. A detailed description of the dynamics that leads to the curves reported in Fig. 2 will be given in the following. From simple textbook calculations, or from more formal analysis like the one made in Ref. [17], it is easy to verify that a localized imaginary potential U induces total reflection as the strength of the potential goes to infinity. Hence the effective quantum dissipation vanishes when the localized imaginary potential is either zero or infinity, implying the existence of a maximum of dissipation for some finite value of U . This explains on a qualitative basis the observed nonmonotonicity. The position of the maximum is of special importance, since it sets the parameters which allow one to engineer the most efficient possible absorbing potential. As an example, in Ref. [17], where the time of arrival of a one-dimensional wave packet is measured by a steplike potential, the maximum dissipation is analytically calculated to be $U_M \approx 10.6E$, where E is the energy of the wave packet. In our case the presence of the nonlinearity and the less idealized conditions do not allow for an analytic solution, but from

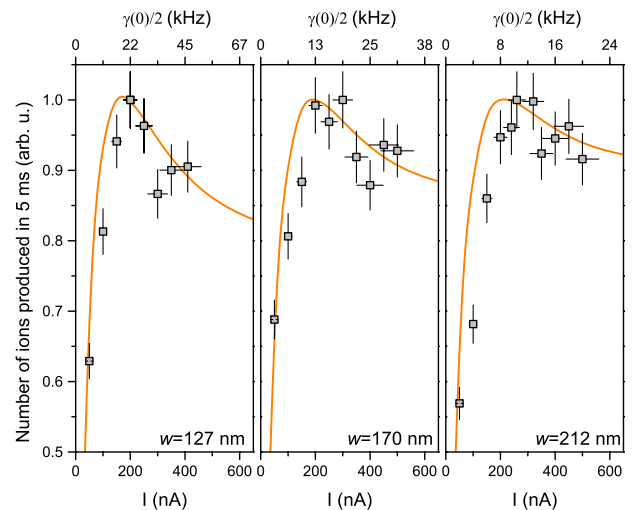


FIG. 2 (color online). Number of ions collected within the first 5 ms of continuous dissipation on a BEC as a function of the EB current I . The three panels report the data obtained with $w = 127(5)$, $170(7)$, and $212(8)$ nm, from left to right. Each data point is the average over 75 experimental repetitions. The error bars are mainly due to shot-to-shot fluctuations in the overall ion detection efficiency. The solid lines are the number of dissipated atoms resulting from the numerical simulations (see text). Please note that in the sum the initial decay visible in Fig. 1(b) is also included. The scale on the top reports the strength of the imaginary potential $U/\hbar = \gamma(0)/2$ corresponding to the measured current.

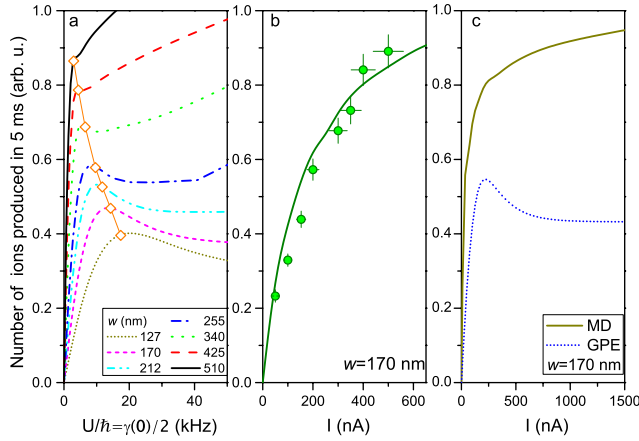


FIG. 3 (color online). (a) Theoretical curves of the number of ions produced in 5 ms as a function of U/\hbar solving Eq. (1) for different values of w . The values of U_M obtained using the approximate expression given in the text are shown as open diamonds over the corresponding curves. (b) Number of ions measured after 5 ms of dissipation for a thermal cloud as a function of the EB current, with $w = 170(7)$ nm. The solid line is the result of the corresponding numerical simulation using the molecular dynamics method. (c) Comparison between the theoretical curves of the number of produced ions as a function of I for the BEC and the corresponding (see text) classical analogue [$w = 170(7)$ nm].

the numerical results plotted in Fig. 3(a) we have found $U_M \approx 8\mu \exp(-w/d)$, where μ and d are respectively the chemical potential and the healing length of the unperturbed BEC. From Fig. 3(a) it also appears that increasing the size of the EB not only moves the position of the maximum dissipation to higher values of I , but also increases the number of produced ions for a given current, and reduces or washes out the effect of the reflection. Clearly, when $U = \hbar\gamma(\mathbf{0})/2 > U_M$, a decrease of the probe size (an increase of the resolution) leads to a lower production of ions, making the system more resistant to the environmental action.

Comparison to classical systems.—To ascertain to which extent our observations are peculiar to the wave nature of the BEC, we have repeated the experiment on a thermal gas of 4×10^5 atoms at $1 \mu\text{K}$ with a beam of $w = 170$ nm. The results are reported in Fig. 3(b), where a simple monotonic behavior is observed. Such data are well reproduced by a classical molecular dynamics simulation, which includes the dissipation induced by the EB [11]. We then extend the classical simulation to an atomic cloud which has the same density, number of atoms, and trapping frequency as our BEC. Even though this does not represent any real physical system, it is instructive to compare the behavior of a quantum system with its hypothetical classical analogue. This comparison is made in Fig. 3(c), where the monotonicity of the classical case is confirmed. From this we can conclude that the observed nonmonotonicity is a purely quantum effect stemming from the macroscopic wave nature of the BEC [18]. Moreover it is evident that

the effect of the quantum reflection from the imaginary potential leads to a suppression of dissipation in the quantum case, which is already notable for very low currents.

Dissipative dynamics.—In order to gain a deeper insight into the dissipation-induced dynamics, we now look in detail at the time-resolved signals coming from the ion detector, reported in Fig. 4(a). Initially the number of ions produced is well described by the exponential decay $\exp(-t\bar{\gamma})$, $\bar{\gamma}$ being the effective dissipation rate [11]. In Fig. 4(b) we show the integral of the signals in the first $5 \mu\text{s}$, together with the simulated values as a function of the EB current. In this phase, where no paradoxical behavior is either observed or expected, the EB burns a hole in the BEC wave function [see Fig. 4(d)], defining a clear border between the space “inside” the hole and that “outside.” Thereafter, the number of ions produced becomes almost constant, signaling the onset of a quasistationary dynamics [19]. In this second phase, the reaction of the quantum system to the external perturbation takes place. When the strength of the dissipation is increased, the “outside” wave function passes from a situation of almost total transmission to a situation where reflection takes the leading role. The nonmonotonic dependence on the dissipation strength then becomes apparent [see Fig. 4(c)]. This represents the first experimental observation of the so-called backflow paradox [20], i.e., of the onset of a temporary reflection from a localized perfect absorber. The curves plotted in Figs. 2 and 3 are then the sum of different contributions like those in Figs. 4(b) and 4(c).

Dissipation as continuous measurement.—Finally we demonstrate that the controlled dissipation is equivalent to a local measurement of the BEC density, i.e., of the squared modulus of its wave function. Starting from Eq. (1) and defining $\phi = \psi/\sqrt{N}$, where N is the number of atoms, after some algebra we obtain the equation

$$\frac{dN(t)}{dt} = -N(t) \int \gamma(\mathbf{x}) |\phi(\mathbf{x}, t)|^2 d\mathbf{x}. \quad (2)$$

The number of ions produced in a time interval Δt around a certain time t is $\Delta N_i(t) = \eta \int_{t-\Delta t/2}^{t+\Delta t/2} |dN(t)/dt| dt$. Hence we can conclude that what we perform is a direct measurement of the BEC density $|\psi(t)|^2$ in the region illuminated by the EB, as in Refs. [14,16]. Since the seminal trilogy on the time of arrival in quantum mechanics [17], imaginary potentials have been linked to the action of a measurement apparatus while later refinements [21] formally demonstrated the equivalence between a pulsed measurement with period δt and a continuous dissipative potential U , provided that $\delta t \approx \hbar/U$. Our findings represent the experimental verification of the equivalence between the action of an imaginary potential and the one of a measurement apparatus on a quantum system. Indeed we show that a continuous measurement of the BEC density is nicely reproduced by introducing an imaginary potential in the

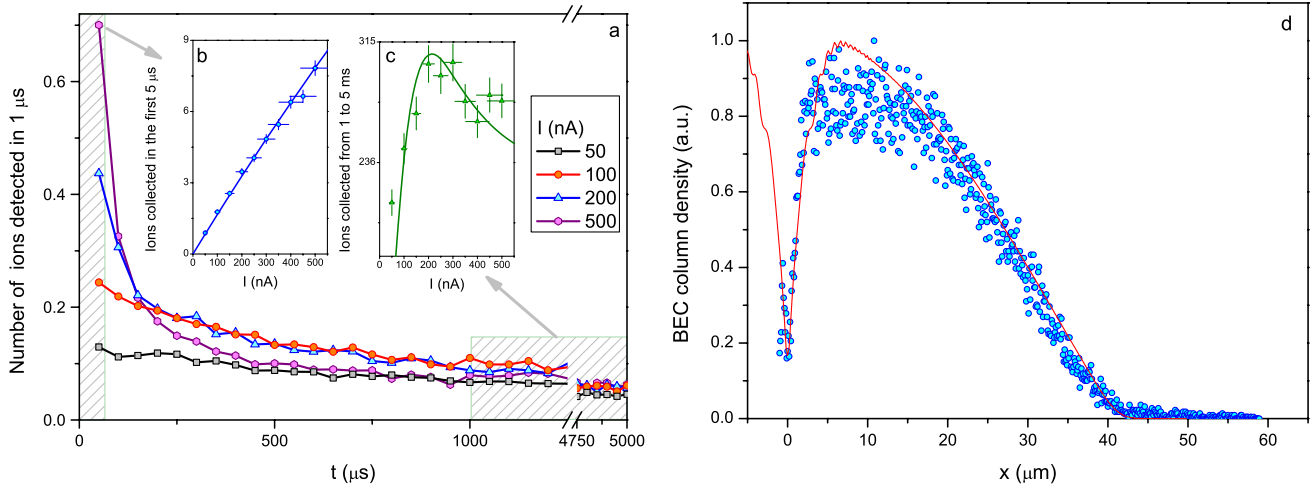


FIG. 4 (color online). (a) Temporal resolved signal of the arrival time of the ions on the ion detector for different values of the EB current I for $w = 170(7)$ nm. In order to enhance readability the data have been plotted with a binning of $50 \mu\text{s}$. The insets (b) and (c) show the integrals of the signal in the shaded areas (the first $5 \mu\text{s}$ and from 1 to 5 ms, respectively) for different values of I together with the theoretical calculations obtained solving Eq. (1). (d) Points: scanning electron microscopy image of the BEC profile along the weak confining axis of the optical trap. The profile is the integrated column density along the direction of propagation of the EB. The scan is made after 1 ms of dissipation. The EB parameters are $I = 150$ nA and $w = 106(5)$ nm. The depletion of the density is visible in the origin, i.e., in the center of the BEC. The solid line is the profile obtained numerically solving Eq. (1).

corresponding Schrödinger equation. Furthermore it is well understood theoretically [22,23], and verified experimentally [24–26], that performing continuous measurements strongly modifies the pre-existing dynamics of a quantum system. This is known as the Zeno (or inverse-Zeno) effect. In general, measurements are mainly performed on nondecaying systems and an extension of the standard definition to such systems is needed. In our case no pre-existing dynamics is present, since in the absence of the EB, the BEC is at rest. We have shown that the action of the continuous dissipative potential, or of the continuous measurement, strongly modifies the output of the measurement itself. In analogy with the standard definition we define dissipation induced Zeno dynamics (DZD) when $dN_i(t)/dU < 0$, $N_i(t)$ being the number of ions produced in the time t , and dissipation induced simple dynamics when $dN_i(t)/dU > 0$. These definitions appear to be the natural extension of the standard ones, since the onset of the DZD requires large values of $U = \hbar\gamma(\mathbf{0})/2$, which corresponds to pulsed measurements with small δt [21]. From the definitions it follows that the dissipation induced simple dynamics is observed where the dynamics is dominated by the Hamiltonian term of the Lindblad master equation, while the onset of the DZD corresponds to a dynamics governed by the dissipative term. We note that an effect resembling the DZD has been observed also in a system of decaying molecules in one dimension [27] and in an attractive Mott-insulator state [28].

Conclusion and outlook.—We have experimentally demonstrated the implementation of an open many-body quantum system whose Hamiltonian and dissipative

dynamics can be independently and accurately controlled. In the case of extremely strong and localized dissipation this can lead to the creation of dissipation-resistant states. The possibility to create such states in a controlled fashion can give new insights for engineering generalized environmental dark states. These kinds of states are of fundamental interest and can possibly have practical applications in quantum computation schemes [29]. And in as much as our technique exploits the demonstrated link between dissipation and measurement, it can be used to address fundamental issues in quantum mechanics, like the definition of the time of arrival [17]. The dissipation mechanism studied in the present Letter is also particularly suited for lattice systems [30], thanks to its localized character and hence to the ability to selectively control the dissipation in a single lattice site. Indeed the use of the EB offers the unique possibility to create and study long-living exotic states in optical lattices [13] and to characterize the interplay between dissipation and interactions (see the Supplemental Material [11] and Refs. [12,31]), and so would give access to the engineering of quantum phases in open quantum systems [32].

We thank J.R. Anglin and A. Widera for reading the manuscript and for fruitful discussions. We are grateful to M. Scholl and P. Würtz for their help in the early stage of the experiment. We also thank V. Konotop and S. Wimberger for enlightening discussions. We acknowledge financial support by the DFG within the SFB/TRR 49 and GRK 792. G.B. and V.G. are supported by Marie Curie Intra-European Fellowships. R.L. acknowledges support by the MAINZ graduate school.

- *barontini@physik.uni-kl.de
- [1] W. Zurek, *Rev. Mod. Phys.* **75**, 715 (2003), and references therein.
- [2] R. Omnés, *Rev. Mod. Phys.* **64**, 339 (1992).
- [3] H. M. Wiseman and G. J. Milburn, *Quantum Measurement and Control* (Cambridge University Press, Cambridge, England, 2010).
- [4] J. T. Barreiro, M. Müller, P. Schindler, D. Nigg, T. Monz, M. Chwalla, M. Hennrich, C. F. Roos, P. Zoller, and R. Blatt, *Nature (London)* **470**, 486 (2011).
- [5] P. W. Shor, *Phys. Rev. A* **52**, R2493 (1995).
- [6] D. G. Cory, M. D. Price, W. Maas, E. Knill, R. Laflamme, W. H. Zurek, T. F. Havel, and S. S. Somaroo, *Phys. Rev. Lett.* **81**, 2152 (1998).
- [7] J. I. Cirac and P. Zoller, *Phys. Rev. Lett.* **74**, 4091 (1995).
- [8] D. A. Lidar, I. L. Chuang, and K. B. Whaley, *Phys. Rev. Lett.* **81**, 2594 (1998).
- [9] A. Beige, D. Braun, B. Tregenna, and P. L. Knight, *Phys. Rev. Lett.* **85**, 1762 (2000).
- [10] R. Stützle, M. C. Göbel, Th. Hörner, E. Kierig, I. Mourachko, M. K. Oberthaler, M. A. Efremov, M. V. Fedorov, V. P. Yakovlev, K. A. H. van Leeuwen, and W. P. Schleich, *Phys. Rev. Lett.* **95**, 110405 (2005).
- [11] See Supplemental Material at <http://link.aps.org/supplemental/10.1103/PhysRevLett.110.035302> for the derivation of Eq. (1), the characterization of the EB, discussions on secondary effects and the effect of the interactions, details on the molecular dynamics simulations.
- [12] V. A. Brazhnyi, V. V. Konotop, V. M. Perez-Garcia, and H. Ott, *Phys. Rev. Lett.* **102**, 144101 (2009).
- [13] D. Witthaut, F. Trimborn, H. Hennig, G. Kordas, T. Geisel, and S. Wimberger, *Phys. Rev. A* **83**, 063608 (2011).
- [14] T. Gericke, P. Würtz, D. Reitz, T. Langen, and H. Ott, *Nat. Phys.* **4**, 949 (2008).
- [15] V. Guarrera, P. Würtz, A. Ewerbeck, A. Vogler, G. Barontini, and H. Ott, *Phys. Rev. Lett.* **107**, 160403 (2011).
- [16] P. Würtz, T. Langen, T. Gericke, A. Koglbauer, and H. Ott, *Phys. Rev. Lett.* **103**, 080404 (2009).
- [17] G. R. Allcock, *Ann. Phys. (N.Y.)* **53**, 253 (1969); **53**, 286 (1969); **53**, 311 (1969).
- [18] Note that the nonmonotonicity could be observed also for thermal particles provided that their wave function is significantly larger than the size of the dissipative potential.
- [19] D. A. Zezyulin, V. V. Konotop, G. Barontini, and H. Ott, *Phys. Rev. Lett.* **109**, 020405 (2012).
- [20] J. G. Muga, J. P. Palao, and C. R. Leavens, *Phys. Lett. A* **253**, 21 (1999).
- [21] J. Echanobe, A. del Campo, and J. G. Muga, *Phys. Rev. A* **77**, 032112 (2008).
- [22] B. Misra and E. C. G. Sudarshan, *J. Math. Phys. (N.Y.)* **18**, 756 (1977).
- [23] A. G. Kofman and G. Kurizki, *Nature (London)* **405**, 546 (2000).
- [24] W. M. Itano, D. J. Heinzen, J. J. Bollinger, and D. J. Wineland, *Phys. Rev. A* **41**, 2295 (1990).
- [25] M. C. Fischer, B. Gutierrez-Medina, and M. G. Raizen, *Phys. Rev. Lett.* **87**, 040402 (2001).
- [26] E. W. Streed, J. Mun, M. Boyd, G. K. Campbell, P. Medley, W. Ketterle, and D. E. Pritchard, *Phys. Rev. Lett.* **97**, 260402 (2006).
- [27] N. Syassen, D. M. Bauer, M. Lettner, T. Volz, D. Dietze, J. J. Garcia-Ripoll, J. I. Cirac, G. Rempe, and S. Dürr, *Science* **320**, 1329 (2008).
- [28] M. J. Mark, E. Haller, K. Lauber, J. G. Danzl, A. Janisch, H. P. Büchler, A. J. Daley, and H.-C. Nägerl, *Phys. Rev. Lett.* **108**, 215302 (2012).
- [29] F. Verstraete, M. W. Wolf, and J. I. Cirac, *Nat. Phys.* **5**, 633 (2009).
- [30] P. Barmettler and C. Kollath, *Phys. Rev. A* **84**, 041606(R) (2011).
- [31] D. Poletti, J.-S. Bernier, A. Georges, and C. Kollath, *Phys. Rev. Lett.* **109**, 045302 (2012).
- [32] M. Müller, S. Diehl, G. Pupillo, and P. Zoller, *Adv. At. Mol. Opt. Phys.* **61**, 1 (2012).